JOURNAL OF CATALYSIS **142**, 499–511 (1993)

Effect of Dilution on 2-Methylpentane Cracking over HY Zeolite

YINGXIAN ZHAO AND B. W. WOJCIECHOWSKI[1]

Department of Chemical Engineering, Queen's University, Kingston, Ontario K7L 3N6, Canada

Received December 1, 1992; revised February 11, 1993

The effect of dilution by N_2 on 2-methylpentane cracking on USHY has been investigated. The results show that dilution inhibits the propagation of certain chain reactions, leading to the shortening of the kinetic chain length and a decrease in the overall rate of feed conversion. Furthermore the total molar selectivity of products increases, resulting in an increased volume expansion. Both the paraffin to olefin ratio and the isomerization to cracking selectivity ratio decrease with increase in the dilution ratio. A quantitative description of the variations of all kinetic parameters, of the reaction pathway probabilities, and of the product formation probabilities with the dilution ratio is presented and the observed behaviour is discussed in terms of the chemistry involved.

INTRODUCTION

Paraffin cracking over zeolite catalysts has been studied over a wide range of systems (*1–12*). Despite this the understanding of the fundamental aspects of this reaction continues to lag behind commercial innovations in cracking catalyst development. Generally, factors which affect the reaction may be divided into two classes: intensive and extensive. The former, such as acid strength, molecular structure, and temperature, can lead to a qualitative change in the reaction mechanism; the latter, such as catalyst to feed ratio and space velocity, normally lead to quantitative changes in the reaction system.

A variety of reactants such as isobutane (*5*), neopentane (*6*), *n*-hexane (*7, 16*), methylpentanes (*4, 13*), *n*-heptane (*14, 15*), *n*-octane (*17*), *n*-nonane (*18*), *n*-dodecane (*19*), and *n*-hexadecane (*20*), as well as various catalysts (*5, 6*) at various reaction temperatures (*18, 21*), have now been studied in order to develop an understanding of the influence of such properties on the reaction mechanism.

The study of other influences is less often used to unravel the mechanism of catalytic cracking. Recently we have reported on a series of studies of 2-methylpentane cracking on HY and presented a chain reaction mechanism to explain the product selectivity, and a kinetic equation to describe the activity in this system (*21*). In the present work we introduce an inert gas, N_2, into the reaction and investigate the effect of dilution ratio, catalyst/feed ratio, and time-on-stream, on the selectivity and kinetics in 2-methylpentane cracking over HY zeolite at 400°C. Although dilution ratio is an extensive property and should only affect quantitative changes, we find that it affects the reaction mechanism in this case.

THEORY

Selectivity

For each reaction product, the time-averaged yield sampled from $t = 0$ to t_f is plotted against the average conversion of feed. Each of these plots is enveloped by a single curve (the OPE), from which the initial selectivity of a product is determined. The details of this methodology have been described in previous literature (*22*).

---

[1] To whom correspondence should be addressed.

0021-9517/93 $5.00

Kinetics

It has been shown that the reaction of 2-methylpentane on HY can be described by the following expression (*21*):

$$\frac{dX}{d\tau} = \frac{A_1\left(\frac{1-X}{1+\varepsilon X}\right) + A_2\left(\frac{1-X}{1+\varepsilon X}\right)^2}{1 + B\left(\frac{1-X}{1+\varepsilon X}\right)} \cdot [\mathrm{SH}]_0(1+Gt)^{-N}. \quad (1)$$

Influence of Dilution on the Variables of the Reaction System

We begin by defining the dependence of various kinetic variables and parameters on the dilution ratio.

Definition of ρ and β. Define the catalyst/oil ratio ρ and dilution ratio β as follows:

$$\rho = \frac{\text{catalyst weight}}{\text{weight of organic reactant}} \quad (2)$$

$$\beta = \frac{\text{moles of nitrogen}}{\text{moles of organic reactant}}. \quad (3)$$

Therefore, the mole fraction of organic feed in the input vapour is given by $1/(1+\beta)$.

Relationship between feed inlet concentration and β. Let $[C_6H_{14}]_{0,\beta}$ represent the initial concentration of feed at dilution ratio β. We relate this to the concentration of pure feed at the same temperature and pressure by

$$[C_6H_{14}]_{0,\beta} = \frac{[C_6H_{14}]_{0,0}}{1+\beta}, \quad (4)$$

where $[C_6H_{14}]_{0,0}$ is the initial concentration of pure feed ($\beta = 0$).

Relationship between the volume expansion coefficient ε and β. Taking 1 mole as a basis and assuming $X = 1$ at $t = 0$ (that is to say, 100% conversion to initial products) gives a measure of the initial volume expansion coefficient ε:

$$\varepsilon_\beta = \frac{(\Sigma n_i) - 1}{1+\beta} = \frac{(\Sigma Y_j) - 1}{1+\beta}. \quad (5)$$

At each dilution ratio the corresponding molar expansion coefficient is obtained by taking $\beta = 0$.

Relationship of kinetic parameters A_1, A_2, and B to β. Assuming that the adsorption and rate constants do not vary with dilution at a given temperature, then using the equations derived for the rate of 2-methylpentane cracking (*21*) and substituting the above developed relationships, we can write

$$A_{1,\beta} = \frac{(\Sigma k_i)K_A(1+\beta) + (\Sigma k_{jR})(\Sigma K_j n_j)[C_A]_0}{(1+\beta) + (\Sigma K_j n_j)[C_A]_0} \quad (6)$$

$$A_{2,\beta} = \frac{-(\Sigma k_{jR})(\Sigma K_j N_j)[C_A]_0}{(1+\beta) + (\Sigma K_j n_j)[C_A]_0} \quad (7)$$

$$B_\beta = \frac{(K_A - (\Sigma K_j n_j)[C_A]_0}{(1+\beta) + (\Sigma K_j n_j)[C_A]_0}, \quad (8)$$

where $[C_A]_0$ is the initial concentration of pure feed. This shows that the kinetics of this reaction can be described at any dilution by obtaining the intensive rate parameters A_1, A_2, etc., and modifying them to account for the dilution ratio β, as long as the n_j values do not vary significantly with dilution.

Relationship among the Variables t_f and τ and the Process Variables ρ and β

It is well established that for fixed bed reactors the feed contact time may be defined by

$$\tau = b\rho t_f. \quad (9)$$

In the presence of diluent gas, Eq. (9) becomes

$$\tau = \frac{b\rho t_f}{1+\beta}. \quad (10)$$

Integrating Eq. (1) with respect to τ at constant t using the boundary condition $X = 0, X$; $\tau = 0, \tau$ (using t_f in Eq. (10)) gives

$$\phi_1 L_n(\phi_2 + \phi_3 X) - \phi_4 L_n(1-X) - \phi_5 X - \frac{b\rho t_f[\mathrm{SH}]_0(1+Gt)^{-N}}{1+\beta} = 0, \quad (11)$$

TABLE 1

Initial Weight Selectivities for Reaction of 2-Methylpentane on HY at 400°C

Product	Dilution ratio				
	0	1	2	3	5
Hydrogen	.0004	.0002	.0002	.0001	.0001
Methane	.0030	.0047	.0064	.0076	.0096
Ethane	.0021	.0023	.0025	.0029	.0030
Ethylene	.0066	.0076	.0088	.0108	.0131
Propane	.0955	.1021	.1033	.1091	.1147
Propylene	.0976	.1088	.1121	.1192	.1277
Isobutane	.0595	.0630	.0650	.0668	.0697
n-Butane	.0229	.0239	.0248	.0265	.0327
C4 olefins	.0117	.0127	.0145	.0193	.0244
Isopentane	.0814	.0821	.0828	.0837	.0857
n-Pentane	.0069	.0073	.0079	.0091	.0109
C5 olefins	.0065	.0079	.0092	.0106	.0158
2,3-Dimethylbutane	.0853	.0809	.0795	.0752	.0690
3-Methylpentane	.4151	.3971	.3858	.3664	.3352
n-Hexane	.0472	.0452	.0440	.0417	.0382
C6 olefins	.0487	.0475	.0472	.0465	.0448
Coke	.0086	.0063	.0048	.0039	.0036
Total	.9990	.9996	.9988	.9994	.9982

where the ϕ_j are the integration constants previously presented in detail (*21*).

Since Eq. (11) is an implicit expression for X, we must determine the cumulative conversion $\overline{X}$ using a numerical method (*18*).

EXPERIMENTAL

The feedstock, 2-methylpentane of 99%+ purity, was obtained from Aldrich and used without further purification. The HY zeolite was prepared from NaY (BDH. Chem., Lot. No. 45912 13Y) (*23*).

All reaction runs were carried out in a fixed-bed gas-phase plug flow reactor. The details of the experimental apparatus and the methodology have been described previously (*17*).

Nitrogen was used as the diluent gas. All products were identified using a Finnigan 1020 GC/MS. Gaseous products were analyzed by a Carle SX 1156 gas chromatograph which allows the direct detection of hydrogen. Liquid products were analyzed by a Varian 3700 gas chromatograph with a capillary column (SE54) and a flame ionization detector. Thermal conversion was subtracted from overall conversion and product yields in the manner described previously (*21*).

Products up to C_7 were eluted at 15°C followed by elution using a temperature program of 5°C/min to 300°C.

RESULTS AND DISCUSSION

The Effect of Dilution on Selectivity

Tables 1 and 2 give the initial selectivities of products at various dilution ratios. We can see that the products include paraffins in the range C_1–C_5, olefins in the range C_2–C_6, three isomers of the feed, hydrogen, and coke at all dilution ratios. The total molar selectivity of all products increases from 1.31 to 1.41 with increase of the dilution ratio from 0 to 5, immediately suggesting that dilution promotes cracking and/or suppresses isomerization.

Effect of dilution on product formation probability (PFP). Figure 1 presents an overall view of PFP of paraffins, olefins, isomers, hydrogen, and coke as these vary with changing dilution ratio. By increasing the dilution ratio from $\beta = 0$ to $\beta = 5$, the sum of the PFPs of both paraffins and olefins

TABLE 2

Initial Molar Selectivities for Reaction of 2-Methylpentane on HY at 400°C

Product	Dilution ratio				
	0	1	2	3	5
Hydrogen	.0172	.0105	.0075	.0063	.0063
Paraffins					
C1	.0161	.0253	.0344	.0409	.0516
C2	.0060	.0066	.0072	.0083	.0086
C3	.1867	.1996	.2019	.2132	.2242
C4	.1222	.1289	.1332	.1383	.1518
C5	.1055	.1068	.1083	.1108	.1154
C6	.5476	.5232	.5093	.4833	.4424
Total paraffins	1.0013	1.0009	1.0018	1.0011	1.0003
Olefins					
C2	.0203	.0233	.0270	.0332	.0402
C3	.1999	.2228	.2295	.2441	.2615
C4	.0180	.0195	.0223	.0296	.0375
C5	.0080	.0097	.0113	.0130	.0194
C6	.0498	.0486	.0483	.0476	.0459
Total olefins	0.2960	0.3239	0.3384	0.3675	0.4045
Coke[a]	.0112	.0075	.0068	.0058	.0057
Total	1.3085	1.3323	1.3470	1.3744	1.4105

[a] Coke molar selectivities were calculated in the manner reported in (*24*).

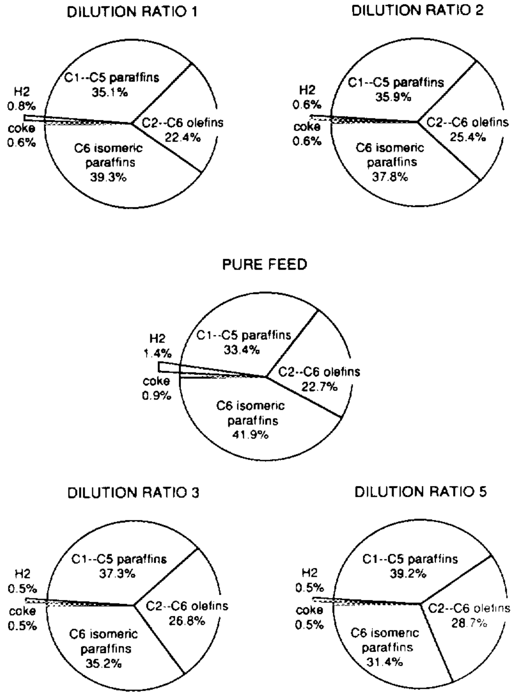

FIG. 1. Product Formation Probability distribution by class: hydrogen, paraffins, olefins, isomers of feed, coke.

increases by about 6% while that of isomers decreases by 10%. The PFPs of coke and H_2, though very small, also decrease with the increase in dilution ratio. Figures 2 and 3 show details of the variation of the PFPs of individual paraffins and olefins with dilution ratio.

Looking at the results in more detail we see that increasing the dilution ratio causes the PFPs of C_1 to C_5 to increase, but in such a way that the size of the product molecule is a factor, so that the PFP of C_5 paraffins stays almost constant while CH_4 formation grows by 300%. For product olefins, the PFPs also increase up to C_5 and decrease for C_6. The above results provide us with evidence that the influence of dilution is different with respect to the rates of the various elementary reactions. The activity of the surface species, the stability of the product, etc., have to be examined individually be-

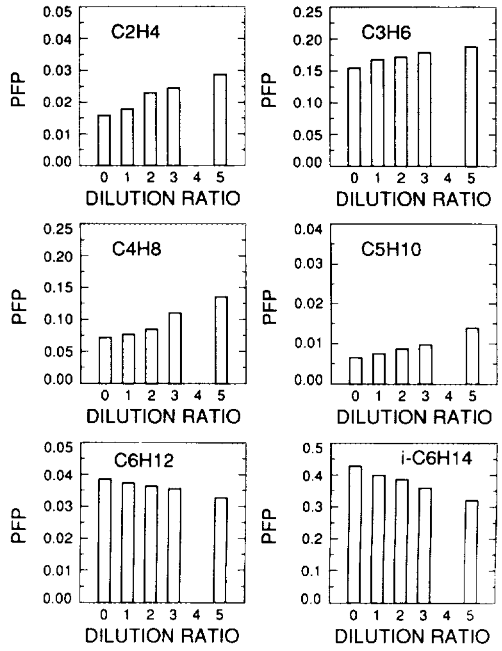

FIG. 2. Product Formation Probability distribution by molecular species: olefins and C_6 isomeric paraffins.

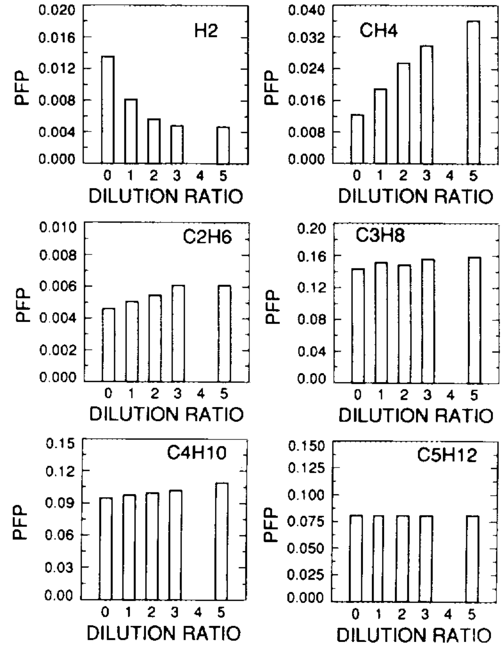

FIG. 3. Product Formation Probability distribution by molecular species: paraffins and hydrogen.

TABLE 3

Reaction Mechanism of 2-Methylpentane on HY Zeolite

Reaction pathway		Type	RPP symbol
$C_6H_{14} + HS$	$\rightarrow H_2 + C_6H_{13}S$	Initiation	X_{00}
$C_6H_{14} + HS$	$\rightarrow CH_4 + C_5H_{11}S$		X_{01}
$C_6H_{14} + HS$	$\rightarrow C_2H_6 + C_4H_9S$		X_{02}
$C_6H_{14} + HS$	$\rightarrow C_3H_8 + C_3H_7S$		X_{03}
$C_6H_{14} + HS$	$\rightarrow C_4H_{10} + C_2H_5S$		X_{04}
$C_6H_{14} + C_2H_5S$	$\rightarrow C_2H_6 + C_6H_{13}S$	Propagation	X_{20}
$C_6H_{14} + C_2H_5S$	$\rightarrow C_3H_8 + C_5H_{11}S$		X_{21}
$C_6H_{14} + C_2H_5S$	$\rightarrow C_4H_{10} + C_4H_9S$		X_{22}
$C_6H_{14} + C_2H_5S$	$\rightarrow C_5H_{12} + C_3H_7S$		X_{23}
$C_6H_{14} + C_3H_7S$	$\rightarrow C_3H_8 + C_6H_{13}S$		X_{30}
$C_6H_{14} + C_3H_7S$	$\rightarrow C_4H_{10} + C_5H_{11}S$		X_{31}
$C_6H_{14} + C_3H_7S$	$\rightarrow C_5H_{12} + C_4H_9S$		X_{32}
$C_6H_{14} + C_4H_9S$	$\rightarrow C_4H_{10} + C_6H_{13}S$		X_{40}
$C_6H_{14} + C_4H_9S$	$\rightarrow C_5H_{12} + C_5H_{11}S$		X_{41}
$C_6H_{14} + C_5H_{11}S$	$\rightarrow C_5H_{12} + C_6H_{13}S$		X_{50}
$C_6H_{14} + C_6H_{13}S$	$\rightarrow C_6H_{14} + C_6H_{13}S$	Isomerization	X_{60}
$C_6H_{13}S^+$	$\rightarrow C_3H_6 + C_3H_7S^+$	β-Cracking	X_{b63}
C_6H_{14}	$\rightarrow m_kC_xH_y + m_hH_2$	Coke Formation	X_{Kc}
$C_2H_5S^+$	$\rightarrow C_2H_4 + HS$	Termination	d_2
$C_3H_7S^+$	$\rightarrow C_3H_6 + HS$		d_3
$C_4H_9S^+$	$\rightarrow C_4H_8 + HS$		d_4
$C_5H_{11}S^+$	$\rightarrow C_5H_{10} + HS$		d_5
$C_6H_{13}^+$	$\rightarrow C_6H_{12} + HS$		d_6

Note. X_{0i} is the probability of feed consumption via the *i*th mode of protolysis mode of initiation; X_{jn} is the probability of feed consumption via the reaction of a feed molecule with the surface ion $C_jH_{2j+1}S^+$ forming a paraffin molecule C_nH_{2n+2} and a new surface ion $C_{6+j-n}H_{2(6+j-n)+1}S^+$; X_{60} is the probability of feed consumption via the production of isomers of the feed molecule; X_{Kc} is the probability of feed consumption by the formation of coke; X_{b63} is the molar selectivity for propylene (C_3) production from the β-scission of $C_6H_{13}S^+$ (C_6) ion; d_j is the molar selectivity for olefin C_jH_{2j} production from the desorption of $C_jH_{2j+1}S^+$ in a termination reaction.

fore we can understand the effect of dilution, or for that matter of catalyst formulation, on the reaction mechanism. To do this we examine the chemical pathways by which various products are formed.

Effect of dilution on reaction pathway probabilities (RPP). In previous work (*24*) we presented a complete chain mechanism to explain 2-methylpentane cracking over HY zeolite. This mechanism consists of three main types of reaction, initiation, propagation, and termination, and each of these includes a set of individual elementary reactions as shown in Table 3. Using this mechanism we have written down the mathematical expressions for this model and calculated the RPPs for the case without dilution by using a suitable computer program (*24*). We now apply the very same equations to the cases with dilution. Figure 4 shows that with increase in the dilution ratio from $\beta = 0$ to $\beta = 5$, the RPP of the sum of initiation reactions, ΣX_{0i}, increases from 29.6% to 40.6%; the RPP of the isomerization reaction, X_{60}, decreases from 54.9% to 44.2%; the RPP of the sum of propagation reactions, ΣX_{jn}, stays almost unchanged, while coke formation, X_{KC}, tends to decrease. Connecting these results to the PFP data we can see why, for example, the ratio of isomerization/cracking decreases with an increase of the dilution ratio, as we find here and as was reported by Corma *et al.* (*14*) in the case of *n*-heptane on an REHY zeolite. Corma *et al.* explained this result by saying that isomerization and cracking require different active sites, in agreement with the work of Daage and Fajula (*10*) and Jacobs and Martens (*25*). The concept of "different acid sites," however, should now be understood to mean something else than different sites on the zeolite framework. Rather than being different by being (a) Brønsted or Lewis sites, (b) the same but of different strength, or (c) acid or free radical sites, the sites differ because the various carbenium ions differ in acidity from the bare proton on the pristine Brønsted acid sites present in the zeolite.

In previous work (*21*, *24*) we proposed that cracking is initiated by the protolysis of C–C and/or C–H bonds in a feed molecule by such pristine Brønsted sites and that isomerization is an integral part of the overall process of cracking in subsequent events identified as chain reactions. In view of the presence of such chain reactions, we can simply and rationally explain the decrease of the RPP of isomerization with increase of dilution as a result of the drop of isomerization rate, due to a decrease in reactant ion concentration on the surface, due to a lower gas phase concentration of the corresponding olefins, caused by the dilution of all hydrocarbon constituents by N_2. The experimental fact that the relative ratio among three isomeric products does not vary with dilution (Table 1 or Fig. 5) implies they are produced from the same "parent" carbeniumion and supports our conclusion.

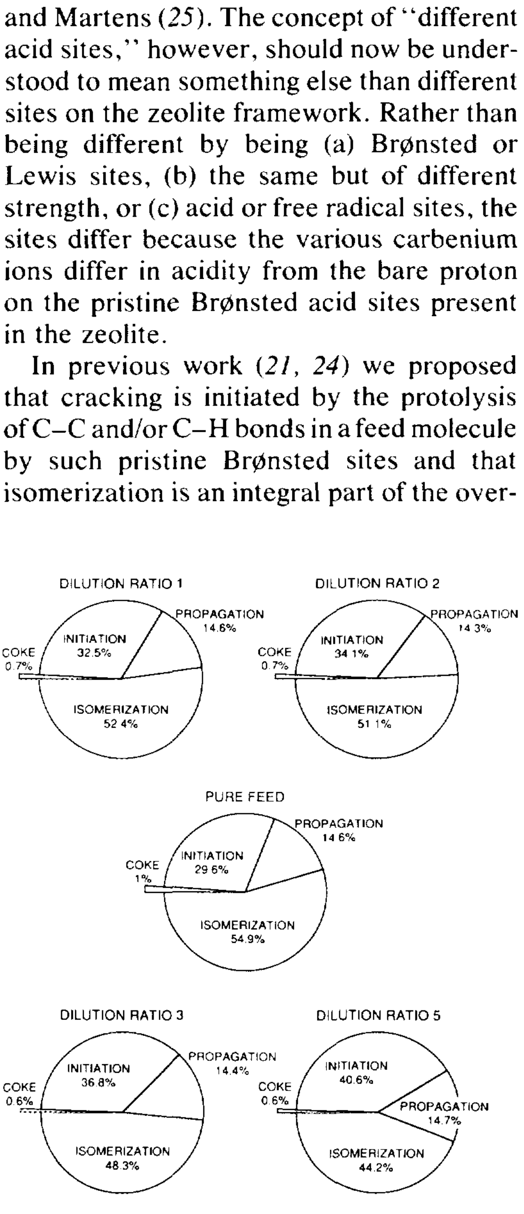

FIG. 4. Reaction Pathway Probability distribution by reaction type: coke formation, initiation, propagation, isomerization.

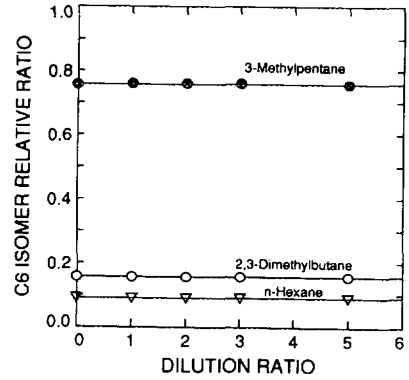

FIG. 5. Ratio of C_6 isomeric paraffins plotted as a function of dilution ratio.

It should be pointed out that the above argument does not mean that acid strength is uniform on the HY surface and all the reaction pathways require the same strength of sites. Exactly the contrary. Figs. 6, 7 show that the RPP of some pathways (X_{20}, X_{21}, X_{31}, X_{40}, X_{41}, X_{B63}) is zero, and that the RPP of other pathways (X_{00}, X_{23}, X_{30}, X_{60}) decreases, while for some (X_{01}, X_{02}, X_{03}, X_{04}, X_{22}, X_{50}) increases with the dilution ratio. These results could be due to the acid strength distribution on the surface, with different reacton pathways requiring different acid strengths.

Effect of dilution on probabilities of bond cleavage by protolysis (*BCP*). We used the

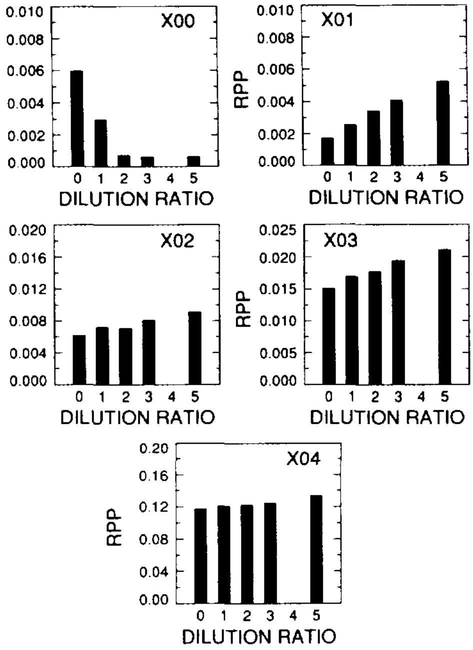

FIG. 6. Reaction Pathway Probability distribution for initiation.

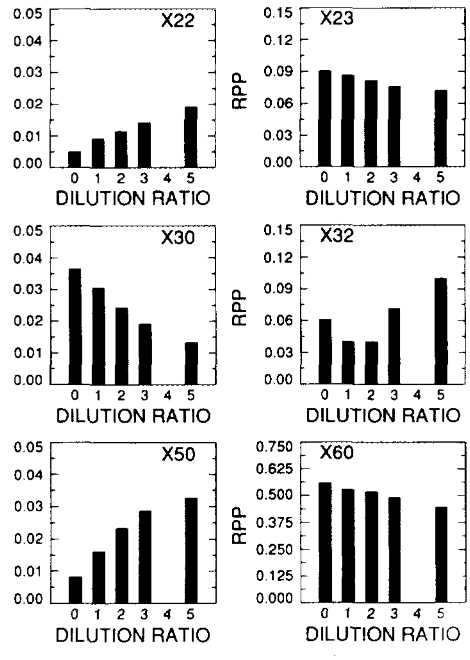

FIG. 7. Reaction Pathway Probability distribution for propagation.

TABLE 4

Effect of Dilution on Probability of Bond Cleavage by Protolysis (BCP)

Broken Bond	BCP Symbol	Dilution Ratio				
		0	1	2	3	5
C_t--C_s	BCP_1	0.510	0.522	0.520	0.528	0.520
C_s--C_s	BCP_2	0.416	0.392	0.379	0.359	0.350
C_t--C_P or C_s--C_P	BCP_3	0.054	0.077	0.100	0.112	0.128
C_t--H	BCP_4	0.020	0.009	0.002	0.001	0.001

term BCP to compare the probabilities of protolysis of various C–C and C–H bonds (*24*). BCP is defined as

$$BCP_i = \frac{RPP_i}{\sum_i RPP_i}. \tag{12}$$

In the absence of dilution the calculated BCP values show the protolysis of bonds in the feed molecule on Brønsted acid sites to obey the following order of preference (*24*):

$$\underset{BCP_1}{C_t—C_s} > \underset{BCP_2}{C_s—C_s}$$

$$> \underset{BCP_3}{C_t—C_p \text{ or } C_2—C_p} > \underset{BCP_4}{C_t—H}$$

Table 4 gives the values of BCPs at different dilution rates. We see that dilution does not change the order of the BCPs, but does change the ratios among them. Increasing the dilution ratio from $\beta = 0$ to $\beta = 5$ caused BCP_1 to stay constant, BCP_3 to increase, and BCP_2 and BCP_4 to decrease. The reason for this is not immediately clear if we are to believe that all the processes represent various kinds of protolysis of the same reactant molecule by the same Brønsted sites. However, if the various modes of protolysis proceed preferentially on sites of specific strength the situation becomes more understandable. In the absence of dilution there is some fraction of Brønsted sites capable of protolysis because they do not have a carbenium ion attached. These sites will have a distribution of acid strengths which is not the same as that on the pristine catalyst but is the result of the steady state achieved between adsorbed species and their gas phase products. This fraction of Brønsted sites gives us the BCP distribution for the catalyst in the absence of dilution. The introduction of a diluent results in the reduction of the fraction of the surface covered by carbenium ions as evidenced by the increase in monomolecular cracking and the decrease in chain cracking. The displaced carbenium ions leave behind Brønsted sites which add to the fraction of Brønsted sites available for carrying out protolysis. Now, if the additional Brønsted sites do not have the same acid strength distribution as those present with no dilution, they will contribute different proportions of the various BCPs.

The reason that hydrogen production, as shown in Table 2, goes down with dilution is clearly connected with the relative probability of the various modes of protolysis shown in Table 4. We argue that more sites are made vacant by the displacement of carbenium ions by the diluent gas. Only the strongest sites are now able to hold on to carbenium ions. This will affect the chain propagating processes. On the other hand protolysis, which proceeds from carbonium ions formed only on the strongest sites, is relatively uninhibited. Only the most difficult reaction of the suite of protolysis processes, the protolysis of a hydrogen atom, is affected negatively. We ascribe this to an interaction between the diluent and the strongest of the strong acid sites capable of promoting protolysis. This interaction has the effect of reducing the strength of such sites, thereby "passivating" their activity. The net effect we observe is that due to a relative decrease in the concentration of sites with the highest strength and hence a decrease in hydrogen production by protolysis. We will be able to discuss this phenomenon more fully when we report on the effects of other diluents.

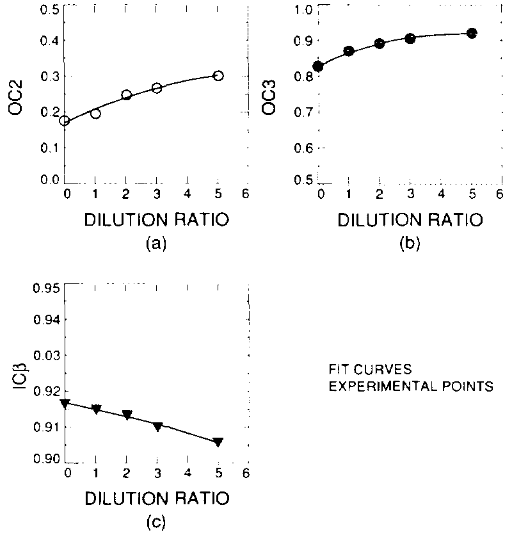

FIG. 8. Effect of dilution on the parallel reactions of surface carbenium ions: $C_2H_5S^+$, $C_3H_7S^+$, and $C_6H_{13}S^+$ at 400°C. (a) OC_2 as a function of dilution ratio; (b) OC_3 as a function of dilution ratio; (c) IC_6 as a function of dilution ratio.

Effect of dilution on the various parallel reactions of surface carbenium ions. In the previous study of pure feed cracking (*24*), we found that the selectivity for those protolysis reactions which produce C_2 and C_3 carbenium ions is 90.5% of all protolysis, and that the selectivity for isomerization of C_6 ions is 79.0% of all the chain reactions. The three carbenium ions which yield these products are therefore the dominant surface species in this reaction system. It is instructive to investigate the various fates which await each of them. There are three kinds of processes which the C_6 carbenium ion may undergo: hydrogen transfer with a feed molecule, desorption as a C_6 olefin, and β-cracking. To compare the probabilities of these processes, we defined

$$IC_6 = \frac{C_6H_{13}S^+ \text{ ion isomerization probability}}{\text{total } C_6H_{13}S^+ \text{ ion reaction probability}}$$

$$IC_6 = \frac{X_{60}}{d_6 + X_{b63} + X_{60}}. \quad (13)$$

Experimental results show that β-cracking plays no role in the conversion of 2-methylpentane at 400°C; i.e., $X_{b63} = 0$. Figure 8c shows that for all dilution ratios the value of $IC_6 > 90\%$ and decreases with increasing dilution ratio. We see this as a tendency of the diluent to displace adsorbed C_6 species before they can isomerize.

To quantify the competition between desorption and propagation for C_2 and C_3 carbenium ions, we similarly define (*24*)

$$OC_2 = \frac{d_2}{d_2 + X_{20} + X_{21} + X_{22} + X_{23}} \quad (14)$$

and

$$OC_3 = \frac{d_3 - X_{b63}}{d_3 - X_{b63} + X_{30} + X_{31} + X_{32}}. \quad (15)$$

In Figs. 8a and 8b we can see that both OC_2 and OC_3 increase with increasing dilution ratio, confirming that dilution promotes desorption or inhibits propagation of bimolecular reactions. Since the C_2 carbenium ion has a higher activity for bimolecular reactions than the C_3 ion (i.e., $OC_2 < OC_3$), it is more sensitive to dilution (i.e., the value of OC_2 changes more rapidly than that of OC_3).

Effect of dilution on the kinetic chain length (KCL). The overall kinetic chain length is defined as the ratio of overall rate to initiation rate. Its value may be calculated from the RPP data using the equation (*24*)

$$KCL = \frac{\sum_i X_{0i} + \sum_n \sum_i X_{jn}}{\sum_i X_{0i}}. \quad (16)$$

The calculated result (Fig. 9) clearly shows that the value of KCL drops from 3.4 to 2.5 with increasing dilution ratio. The result is in agreement with purevious discussion since dilution promotes initiation and termination reactions while it impedes propagation by encouraging desorption.

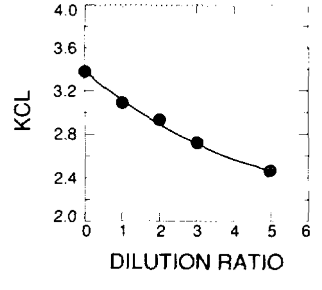

FIG. 9. Kinetic chain length plotted as a function of dilution ratio.

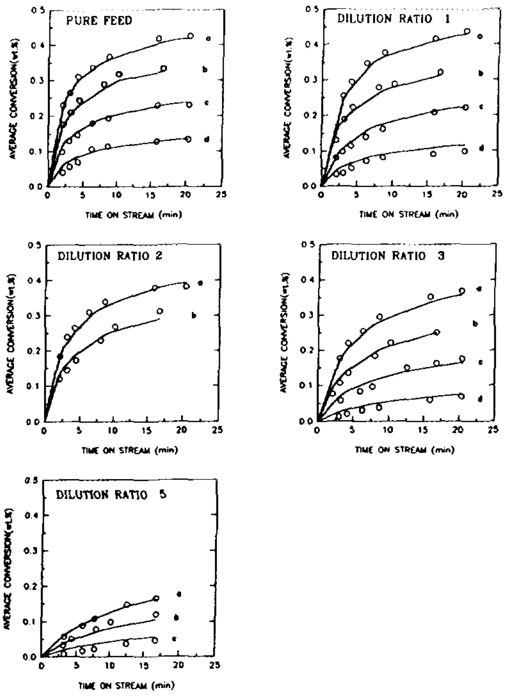

FIG. 10. Fit conversion curves and experimental points for 2-methylpentane cracking on HY at 400°C. Catalyst-to-reactant ratios: (a) 0.11, (b) 0.068, (c) 0.035, (d) 0.013. Dilution ratios are 0, 1, 2, 3, and 5.

The Effect of Dilution on Conversion

Figure 10 show the behaviour of the cumulative conversion as a function of the final time on stream t_f. The parameter for each curve is ρ, the catalyst-to-feed weight ratio. The five graphs vary as the diluent-to-feed molar ratio, β, is changed from 0 to 1 to 2 to 3 to 5. For each curve in the figures, a limiting conversion is approached at long time on stream. The level of limiting conversion is governed by ρ. The larger the ρ value, the higher the level of the limiting conversion, and the steeper the curve in the portion at short time-on-stream. These results show, in a qualitative way, the dependence of reaction rate on the number of active sites.

According to the TOS theory (*22*, *26*), the deactivation of the catalyst in this system should belong to Class II, with a decay exponent of $N = 1$ in the TOS decay function:

$$\theta = (1 + Gt)^{-N}. \tag{17}$$

The addition of a diluent to the reacting system not only decreases the partial pressure of feed leading to a decrease in the reaction rate, but also decreases the rate of catalyst decay. In Fig. 11 this leads a crossing of conversion curves, a phenomenon which could easily generate confusion if the reaction system is studied in a narrow range of conditions. In particular we should remember that the opposite effects we observe here by reducing the partial pressure of the reactant will also occur if we decrease reaction pressure using pure reactant.

The Effect of Dilution on Kinetic Parameters

The experimental conversion data have been fitted by Eq. (1) (see Fig. 10). Optimum values of the kinetic parameters A_1, A_2, B, G, and ε are presented in Table 5. One can see that the values of A_1, A_2, and B increase, and those of G and ε decrease with increasing dilution ratio.

TABLE 5

Effect of Dilution on Kinetic Parameters for Reaction of 2-Methylpentane on HY at 400°C

Dilution N2/feed	A_1 (min^{-1})	A_2 (min^{-1})	B	G (min^{-1})	N[a]	ε[b]
0/1	0.267	−0.0838	−0.902	0.262	1	0.309
1/1	0.308	−0.0771	−0.850	0.232	1	0.166
2/1	0.403	−0.0709	−0.731	0.224	1	0.116
3/1	0.498	−0.0626	−0.663	0.208	1	0.094
5/1	0.567	−0.0517	−0.605	0.189	1	0.068

Note. Although *overall* volume expansion, ε, decreases with dilution ratio as shown above, the volume of *products per mole of reactant coverted* increases as shown by the increase in total moles produced in Table 2.

[a] N is fixed at 1 (Ref. (*22*)).

[b] ε is calculated as in Eq. (5).

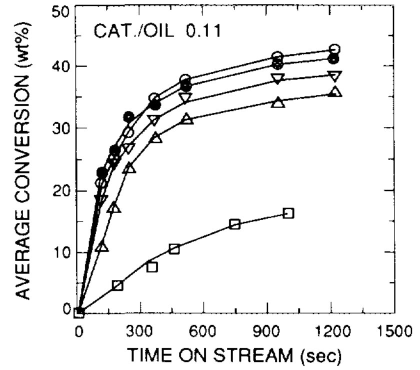

FIG. 11. A plot of average conversion as a function of time on stream at catalyst-to-reactant ratio of 0.11 and at 400°C. Dilution ratio: (●) 0; (○) 1; (▽) 2; (△) 3; (□) 5.

Defining $I = \Sigma K_j n_j [\mathrm{C_A}]_0$ and assuming I to be independent of β, from Eqs. (6) and (8) we may write the ratio

$$\frac{A_{2,0}}{A_{2,\beta}} = \frac{B_0}{B_\beta} = 1 + \left(\frac{\beta}{2 + I}\right), \tag{18}$$

while from Eqs. (6) and (7) we have

$$\frac{1}{A_{1,\beta} + A_{2,\beta}} = \frac{I}{\Sigma k_i K_{\mathrm{A}}(1 + \beta)} + \frac{1}{\Sigma k_i K_{\mathrm{A}}} \tag{19}$$

and

$$\frac{A_{1,\beta} + A_{2,\beta}}{A_{2,\beta}} = \frac{\Sigma k_i K_{\mathrm{A}}}{I \Sigma k_{j\mathrm{R}}}(1 + \beta). \tag{20}$$

Using the parameters in Table 5, we have drawn Fig. 12. From the intercept and/or slopes of these linear plots we have calculated the adsorption and rate constants (Table 6). The development of the pertinent mathematics is presented in the Appendix. From Table 6 we see that $K_{\mathrm{A}}/\Sigma n_j K_j = 2.12 \times 10^{-3}$, showing that carbenium ions are much more stable than carbonium ions on the catalyst surface. Also $\Sigma k_i / \Sigma k_{j\mathrm{R}} = 12.45$ mol/liter, implying that the specific rate of reaction of carbonium ion protolysis is greater than that of carbenium ions reacting with feed molecules. However, since the rate of a heterogeneous reaction de-

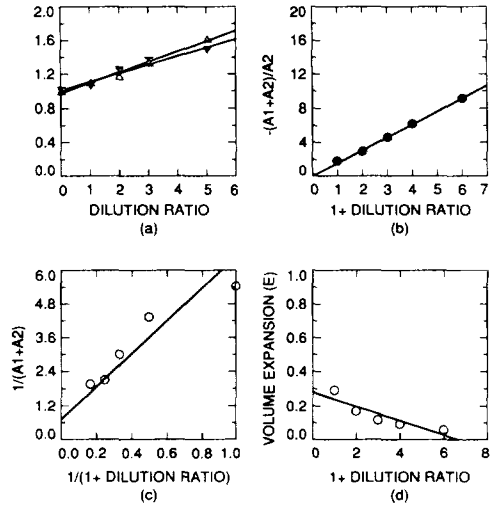

FIG. 12. Effect of dilution on kinetic parameters: (a) $A_{2,0}/A_{2,\beta}$ and B_0/B_β as functions of dilution ratio β; (b) $-(A_{1,\beta} + A_{2,\beta})/A_{2,\beta}$ as function of $1 + \beta$; (c) $1/(A_{1,\beta} + A_{2,\beta})$ as a function of $1/(1 + \beta)$; (d) ε as a function of $1 + \beta$.

pends not only on the rate constants but also on the concentrations of active surface species and the concentration of reactant in the gas phase, the chain processes involving carbenium ions are actually responsible for more of the conversion than are the carbonium ions.

The variation of the volume expansion factor, ε, with dilution (Table 5) is described by Eq. (5) and shown in Fig. 12d. We see that the influence of dilution on the total product selectivity is not very large, though we saw that the selectivity distributions with respect to individual products change significantly.

The decay parameter G decreases with increasing dilution ratio, indicating that dilution affects the decay of the catalyst. This effect will be examined in more detail in the future but it is thought to be related to the reduction of surface coverage by carbenium ions.

CONCLUSIONS

The introduction of an inert diluent gas, N_2, into the reaction of 2-methylpentane on HY reduces the gas phase concentration of the reactant and adjusts the acid strength distribution of the unoccupied Brønsted sites on the catalyst surface. As a consequence increasing dilution ratio results in:

1. An increase in the PFPs of the smaller products and an increase in the sum of the product molar selectivities, i.e., dilution results in greater volume expansion and in a smaller average product molecular weight.
2. An increase in the RPPs of initiation and a decrease in the RPPs of isomerization together with little or no change in the RPPs of other forms of propagation. This results in a decrease in the ratio of paraffins to olefins and a smaller selectivity for isomerization.
3. A change in the relative bond cracking probabilities (BCP) distribution with no change in the order of BCP_i. This fact suggests that the sites responsible for protolysis are somehow different at the various levels of dilution. We believe that this difference is a result of the change in the number of sites available for protolysis. If a range of site acid strengths exists and takes part in

TABLE 6

Adsorption and Rate Constants for Reaction of 2-Methylpentane over HY Zeolite at 400°C

K_A (liter/mol)	$\Sigma n_j K_j$ (liter/mol)	$K_A/\Sigma n_j K_j$	Σk_i (mol/liter/min)	Σk_{jR}	$\frac{K_A \Sigma k_i}{\Sigma n_j K_j [C_A]_0 \Sigma k_{jR}}$
1.11	523	2.12×10^{-3}	1.37	0.11	1.48

Note. The method of calculation is presented in the Appendix.

protolysis then it would be expected that various acid strengths show preferential activity with respect to the protolysis of specific bonds. As the total number of empty sites changes so does their acid strength distribution, and so the BCP.

4. Promotion of the desorption of carbenium ions and a shortening in the reaction chain length. These effects are the ones responsible for the changes in the number of protolysis sites and in the distribution of their acid strengths.

5. Reduction in the overall rate of reactant conversion. This results from the reduction in the rate of conversion due to chain processes. This rate decrease is partially compensated by the increase of protolysis on the vacated sites but the net result is a lower overall rate of conversion.

6. Lowering of the rate of catalyst decay. Since fewer sites remain occupied by carbenium ions at high dilution, there is less chance for bimolecular reactions between adjacent carbenium ions. We believe such reactions to be at least partially responsible for the formation of dehydrogenated species found in coke and hence responsible for catalyst decay.

APPENDIX I

1. Calculation of Adsorption Constants

From Fig. 12a the slope of the curves is 0.096. Equation (18) gives

$$\Sigma n_j K_j [C_A]_0 = I = 1/0.096 - 1 = 9.42. \quad \text{(A1)}$$

From Eq. (8) and inserting $B_0 = -0.902$ and $I = 9.42$, we have

$$K_A [C_A]_0 = B_0(1 + I) + I = 0.02. \quad \text{(A2)}$$

Combining Eqs. (A1) and (A2), we obtain:

$$K_A/\Sigma n_j K_j = 0.02/9.42 = 2.12 \times 10^{-3}. \quad \text{(A3)}$$

Reactions have been carried out at 1 atm and 400°C, that is,

$$[C_A]_0 = 0.018 \text{ mol/liter}, \quad \text{(A4)}$$

and hence

$$K_A = 1.11 \text{ liter/mol} \quad \text{(A5)}$$

$$\Sigma n_j K_j = 523 \text{ liter/mol}. \quad \text{(A6)}$$

2. Calculation of Rate Constants

From Fig. 12b we measure the intercept as 0.66. Equation (19) gives

$$K_A \Sigma k_i = 1/0.66 = 1.52 \text{ min}^{-1}. \quad \text{(A7)}$$

Combining with Eq. (A5) we have

$$\Sigma k_i = 1.37 \text{ mol/liter/min} \quad \text{(A8)}$$

From Fig. 12c we measure the slope of the curve as 1.48. Equation (20) gives

$$K_A \Sigma k_i \Sigma n_j K_j [C_A]_0 \Sigma k_{jR} = 1.48. \quad \text{(A9)}$$

Combining Eq. (A9) with (A7) and (A1), we obtain

$$\Sigma k_{jR} = 0.11 \text{ min}^{-1}. \quad \text{(A10)}$$

APPENDIX II. NOMENCLATURE

X	instantaneous fractional conversion of feed (dimensionless)
$\overline{X}$	average fractional conversion (dimensionless)
τ	space time (min)
t	catalyst time-on-stream (min)
t_f	total run time of the experiment (min)
ε	volume expansion
Θ	fraction of active sites remaining at time t
G	aging parameters (min^{-1})
N	aging exponent (dimensionless)
A_1, A_2, B	kinetic parameters
$[SH]_0$	concentration of active sites (initial)
ρ	catalyst to oil weight ratio (dimensionless)
β	diluent gas (N_2) to feed mole ratio (dimensionless)
b	reactant to catalyst density ratio (dimensionless)
ϕ_j	integration constant
$[C_6H_{14}]_0$ or $[C_A]_0$	initial concentration of reactant (mol/L)

n_i	number of moles of product *i* when 1 mole of feed is completely converted
ΣY_j	sum of the molar selectivities of products when 1 mole feed is completely reacted
K_A	adsorption constant of reactant
K_j	adsorption constant of the *j*th product
k_i	rate constant of the *i*th mode of monomolecular reaction
k_{jR}	rate constant of carbenium ion $C_jH_{2j+1}S^+$ undergoing the Rth mode of bimolecular reaction
PFP	product formation probability
RPP	reaction pathway probability
BCP	bond cleavage probability (by protolysis)
KCL	kinetic chain length

REFERENCES

1. Wojciechowski, B. W., and Corma, A., "Catalytic Cracking." Dekker, New York, 1986.
2. Mole, T., and Anderson, J. R., *Appl. Catal.* **17,** 141 (1985).
3. McVicker, G. B., Kramer, G. M. and Ziemiak, J. J., *J. Catal.* **83,** 286 (1983).
4. McVicker, G. B., Kramer, G. M., and Ziemiak, J. J., *J. Catal.* **92,** 355 (1985).
5. Lombardo, E. A., and Hall, W. K., *J. Catal.* **112,** 565 (1988).
6. Lombardo, E. A., Sill, G. A., and Hall, W. K., *J. Catal.* **119,** 426 (1989).
7. Abbot, J., and Wojciechowski, B. W., *Can. J. Chem. Eng.* **66,** 825 (1988).
8. Abbot, J., and Wojciechowski, B. W., *J. Catal.* **113,** 353 (1988).
9. Daage, M., and Fajula, F., *J. Catal.* **81,** 100 (1983).
10. Daage, M., and Fajula, F., *J. Catal.* **81,** 394 (1983).
11. Corma, A., Fornes, V., J. B., and Orchilles, A. V., *Appl. Catal.* **12,** 105 (1984).
12. Corma, A., Planelles, J., and Tomas, F., *J. Catal.* **94,** 445 (1985).
13. Abbot, J., *Appl. Catal.* **57,** 105 (1990).
14. Corma, A., Monton, J. B., and Orchilles, A. V., *Appl. Catal.* **23,** 255 (1986).
15. Maatman, R., Friesema, C., Mellema, R., and Maatman, J., *J. catal.* **47,** 62 (1977).
16. Borade, R. B., Hegde, S. G., Kulkarni, S. B., and Ratnasamy, P., *Appl. Catal.* **14,** 27 (1984).
17. Abbot, J., and Wojciechowski, B. W., *J. Catal.* **107,** 451 (1987).
18. Groten, W. A., and Wojciechowski, B. W., *J. Catal.* **140,** 262 (1993).
19. Abbot, J., and Wojciechowski, B. W., *J. Catal.* **115,** 1 (1989).
20. Abbot, J., and Wojciechowski, B. W., *J. Catal.* **109,** 274 (1988).
21. Zhao, Y. X., Bamwenda, G. R., Groten, W. A., and Wojciechowski, B. W., *J. Catal.* **140,** 243 (1993).
22. Wojciechowski, B. W., *Catal. Rev. Sci. Eng.* **9**(1), 79 (1974).
23. Groten, W. A., and Wojciechowski, B. W., *J. Catal.* **122,** 362 (1990).
24. Zhao, Y. X., and Wojciechowski, B. W., *J. Catal.*, in press.
25. Jacobs, P. A., and Martens, J., *in* "Acids and Bases as Catalysts, Lyon, 1984."
26. Wojciechowski, B. W., *Can. J. Chem. Eng.* **46,** 48 (1968).